

# Deciphering Motion Signatures of *Escherichia coli* under Ampicillin and Polymyxin B Stress: A Multidimensional Approach Using Optical Flow and Angular Profiling

Ali Adel DAWOOD<sup>1</sup>, Zayd Kays OMER<sup>2</sup>, Mohanad Adnan MOHAMMED<sup>3</sup>

## Abstract

This study is a multidimensional research of *Escherichia coli* genetically paralyzed by ampicillin and polymyxin B using optical flow, Gaussian Mixture Model (GMM) clustering, angular profiling and fluorescence estimating. Phase sensitive microscopy and quartz crystal resonators provided an opportunity to efficiently monitor bacterial responses on a mechanical and visual level simultaneously. Optical flow Farneback was used to extract motion vectors that were clustered and discussed in terms of displacement, directionality and angular distribution. The samples treated with ampicillin had a heterogeneous motility in which the clusters have a high speed and directional bias along the Z-axis. In comparison, polymyxin B samples contained uniformly suppressed samples of the low-speed clusters with low angular bias. Motion mapping of HSV visualized forms of movement was done on the basis of color coded and fluorescence analysis was done to determine the metabolism of the motile clusters. The novelty of the given work lies in the fact that it involves the use of both mechanical and optical cues in the process of revealing antibiotic-specific motion patterns and organized angular reactions. These observations suggest that not only motion of bacteria under stress is suppressed but this motion is conditionally and complexly regulated. The proposed approach will deliver the speed of diagnostics and live resistance profiling.

**Keywords:** Antibiotic Effects; Angular and Cluster Profiling; Bacterial Motility; *E. coli*; Optical Flow Analysis;

<sup>1</sup>Department of Anatomy, Al-Batool College of Medicine, University of Mosul, Mosul, Iraq

<sup>2</sup>Department of Physiology, Al-Batool College of Medicine, University of Mosul, Mosul, Iraq

<sup>3</sup>Department of Anatomy, Al-Batool College of Medicine, University of Mosul, Mosul, Iraq

**\*Corresponding author:**

**Ali Adel DAWOOD**, Department of Obstetrics and Gynecology, College of Medicine, University of Baghdad, Baghdad, Iraq

**E-mail:** aad@uomosul.edu.iq

## INTRODUCTION

Bacterial motility is a biological feature that can be considered one of the primary abilities of microorganisms to explore their surroundings, to respond to chemical gradients and to survive. There are a host of different mediators of such locomotion, such as flagellar propulsion, twitching via type IV pili, gliding and swarming behavior, which are different structural and regulatory pathways<sup>1,2</sup>. Motility is not only a survival strategy, but also in the center of host colonization, biofilm and pathogenesis and consequently, has now become of central concern in the study of the environment and also in clinical research<sup>3,4</sup>.

Recent advances in microscopy and computational analysis now permit observation of bacterial behavior in high-resolution, and have demonstrated that not all complex behavioral patterns can be readily obtained. The individual cell motility can be determined to provide insight into the physiology of the bacteria, chemotactic dynamics and heterogeneity of a population<sup>5</sup>. Additionally, motion analysis has proven to be a powerful method in studying the action of antibiotics because they tend to change their motile activity preceding morphological changes or cell death occurred and this can act as an early signal of antimicrobial action<sup>6,7</sup>.

The technique of tracking and comprehension of bacterial motions has extensive applications. Clinical diagnostics can be used to do rapid susceptibility test and resistance profiling based on motion-based metrics, especially with optical biosensors or microfluidic systems with them<sup>8</sup>. The behavior of microorganisms that inhabit the complex environment (e.g., soil, water, parasite niches, etc.) can be explained using motility tracking in environmental microbiology<sup>9</sup>. Synthetic biology also includes motion measurement, where engineered bacteria are programmed to accomplish particular tasks, such as pollutant removal or drug delivery, and locomotion in this case has to be tightly regulated<sup>10</sup>.

The quantification of motion has been revolutionized by the technological inclusion of the optical flow algorithms, clustering and the angular profiling. Large datasets can also be analyzed with tools such as RABiTPy and neural network-based segmentation pipelines, which can scale and be replicated to analyze large datasets and provide a solution over the limitations of manual tracking and the ability to make powerful statistical comparisons between conditions<sup>11,12</sup>.

The developments have brought about multidimensional motion analysis whereby a mechanical movement is correlated with biochemical activity and genetic regulation<sup>13</sup>.

Notably, bacterial motility is currently being acknowledged as a regulator of the development of antibiotic resistance. Experiments have also demonstrated that motile cells can avoid high-concentration zones, postpone exposure and promote horizontal gene transfer, which increases the speed of resistance formation in spatially heterogeneous situations<sup>14</sup>. The knowledge of these dynamics is critical to the design of effective antimicrobial strategies and forecasting patterns of resistance<sup>15,16</sup>.

With this in mind, this paper will design and implement a multimodal mechanism of measuring the motion of bacteria when under the influence of antibiotics. With the combination of clustering, angular profiling and HSV-based optical flow images, we will aim to describe ampicillin and polymyxin B motility signatures. It is aimed at discovering new behavioral trends that can be used as early warning signs of antibiotic action and develop motion-based measurements as the supplementary instrument of microbiological studies and diagnostics.

## MATERIALS AND METHODS

### Bacterial strain and motility verification

The data about the gathered strains and videos were received in<sup>17</sup>. Genetically paralyzed flagella were used in *Escherichia coli* HCB136. This strain was one of the gifted ones by Howard Berg lab at Harvard University. A motility agar test was done to ensure that there was no motility by inoculating a 0.2 percent of media (Hardy Diagnostics, cat. no. Q11). HCB136 in this assay grew solely at the stab site and did not move using flagellation. Motile *E. coli* K12 (ATCC 23716) was used as a positive control and this showed diffuse radial growth projecting outward of the stab site. The verification was necessary to ascertain that whatever motion observed in later experiments was not because of intrinsic motility, but because of external stimuli or mechanical responses due to antibiotics.

### Procedure regarding antibiotic exposure

On confirmation, the bacterial cultures were subjected into two antibiotics with different modes of action Ampicillin (100 µg/mL) and Polymyxin B (200 µg/mL) were added at specified times to determine the inhibition of motility.

### Video images and data gathering

Monitoring of bacterial responses was done by the use of phase sensitive optical microscopy coupled with a quartz crystal resonator (QCR). This apparatus allowed the simultaneous visualization of bacterial motion and measurement of mechanical variations of nanoscale by measuring the phase noise. The videos were made under fluorescence and both spatial and temporal variation of bacterial behavior was recorded. The videos were recorded at six frames per second and had 1392 x 1040 pixels' resolution and an area of view that was about 0.024 mm<sup>2</sup>. The length of individual recording sessions was about 120 frames, which is adequate to provide a time resolution that is capable of highlighting the dynamic variations in bacterial behavior after exposure to antibiotics.

### Combination of mechanical and optical signaling

The quartz crystal resonator was a mechanical sensor and a bacterial adhesion substrate. The mechanical vibrations of the bacteria were measured by causing a shift in the phase noise of the resonator as the bacteria contacted the crystal surface and were recorded in parallel with the optical video data. The two-modal system made it possible to correlate mechanical activity with visual motion patterns, which provided a high-resolution system of measuring bacterial responses to antimicrobial stress. The videos that were obtained then formed the foundation of motion analysis, clustering, and statistical analysis.

### Motion vector extraction and data preparation

Farneback optical flow was used to extract motion vectors (dx, y) and track the displacement of the bacteria on a frame-by-frame basis. These motion vectors are accumulated to each of the tracked bacteria in the video and stored in a formatted format. The vectors are then transformed to a NumPy array to enable clustering and statistical analysis of each row of the array representing the movement of an individual bacterium:

Column 1: horizontal displacement (dx)

Column 2: vertical displacement (dy)

This array serves as the input for subsequent modeling.

### Clustering motion patterns using Gaussian Mixture Model (GMM)

In order to determine unique behavior patterns during bacterial motion, we use a Gaussian Mixture Model (GMM). This statistical model is based on the assumption that the data is created as a result of a combination of numerous Gaussian distributions which

are associated with the various clusters of movement behavior.

Trying to preserve continuity, cluster identities (0, 1, 2) were always color-coded all through. The number of clusters (e.g. 2 or 3) is specified by us depending on how varied we expect this dataset to be. The GMM algorithm is used to fit the model to the data on motion and allocate every vector to one of the clusters. The classification is defined by the probability of a certain vector of a specific Gaussian component. The clustering process assists in isolating bacteria into the following groups: Non-motile or dead cells; Weakly motile or stressed cells; Actively motile or resistant cells.

Every bacterium will be identified with a cluster index, which will be later identified during visualization and statistical comparison.

The scatter plot gives a picture of the distribution of the motion data and the ability to distinguish between different patterns of movement that has been achieved by the GMM. It also enables us to see the spread, density and orientation of every cluster in the displacement space.

The axes are: X-axis: horizontal motion (dx); Y-axis: vertical motion (dy).

The visualization of the clustering results is important to the interpretation of the clustering results and the establishment of the potential biological significance.

### Quantifying cluster characteristics

To understand the nature of each cluster, we compute statistical metrics for the motion vectors within each group. These include:

**Mean displacement:** average values of dx and dy for each cluster, indicating the general direction and magnitude of movement.

**Standard deviation:** measures the variability of displacement within the cluster, reflecting how consistent or scattered the movements are.

**Cluster size:** the number of vectors assigned to each cluster, which may correlate with the proportion of bacteria exhibiting a specific behavior.

### Directional analysis using vector plots

Directional changes of motion vectors were measured with spectral angle analysis especially when there is an antibiotic stress. we employ the vector plots (quiver plots). In these plots, every motion vector is traced as an arrow which has the origin (0, 0) and which points to the displacement (dx, dy) of a bacterium.

This technique gives an opportunity to observe the magnitude and the direction of movement as well.

The grouping of vectors in clusters with unique colors would allow us to test the hypothesis of directional bias or random dispersion of particular clusters. The plot maintains the spatial proportions and grid lines and equal axis scaling to make the proper interpretation. It is especially applicable to detection of a coordinated movement, chemotaxis or escape behavior.

### Profiling of angular motion during experimentation in presence of antibiotics

Angular displacement data of each of seven experimental units were extracted to research the directional motion patterns during antibiotic treatment. The units were biological or experimental conditions and the movement was examined in three spatial directions viz. X, Y, and Z. These data were divided into two groups Units 1-4 were marked with Ampicillin and Units 5-8 were marked with PMB. Angular distributions were generated per unit, in eight biological classes (i.e. representing various populations of bacteria or molecules). The values were plotted in the form of density curves to see the frequency and the direction of movement by the classes and axes.

### Motion vector-based clustering and angular feature extraction

In order to describe the bacterial motion under the influence of the antibiotics, directional vectors ( $dx_1$ ,  $dx_2$ ) were obtained out of the video frames and applied to calculate speed and angular orientation. Speed was determined as ( $Speed = \sqrt{dx_1^2 + dx_2^2}$ ) and angle was determined as:  $Angle = \arctan_2(dy, dx)$ . GMM was used to detect latent clusters in the data and scatter plots made to visualize the spatial distribution of each cluster. Also, spectral angle (SA) measures were calculated on 100 biological classes to compute directional similarity and evaluate the effect of ampicillin treatment.

Farneback Optical Flow HSV-encoded dense motion mapping (HEDMM-FBOF).

HEDMM-FBOF would allow tracking the movement of bacteria at pixel level and detecting the hidden vibrations. To measure the movement of bacteria under antibiotic action, we adopted dense optical flow method with Farneback algorithm then color-based coding in Hue Saturation Value (HSV) space. The images are color-coded which results in an intuitive interpretation: the red or pink color denotes horizontal movement, the blue or cyan color denotes vertical movement, the green or yellow color denotes mixed or rotational movement, and the dark spots are the ones corresponding to non-motile or still cells.

The Farneback algorithm compares movement among sequential video images based on modeling the local difference of intensity of every image section as a quadratic constancy. to be more precise, the value of  $I(x)$  at one-pixel position  $xx$  is argued to be in the form of:

$$I(x) \approx x^T A x + b^T x + c$$

where  $A$  is a symmetric matrix representing the curvature of the intensity surface,  $b$  is the gradient vector, and  $c$  is a constant offset. By comparing these polynomial coefficients across two frames, the algorithm computes the displacement vector:

$\vec{v}^T(x, y) = (dx, dy)$  for each pixel, capturing both horizontal and vertical motion components.

To visualize these motion vectors, we transformed them into a color-coded image using the HSV model. The direction of motion is encoded in the hue component, calculated as:

$$\theta = \arctan_2(dy, dx)$$

This angle  $\theta$  represents the orientation of movement, with different hues corresponding to horizontal, vertical, diagonal, or rotational motion. The magnitude of the displacement vector, representing the speed of movement, is computed as:  $|\vec{v}^T| = \sqrt{dx^2 + dy^2}$

This value is converted to brightness (value) channel of the HSV space where brighter pixels mean a higher speed of motion. The saturation is normally adjusted to its highest level so that it becomes more distinctive. The last HSV photo is transformed into RGB to be shown and it results in a pseudo-fluorescent image of bacterial behavior.

It is a methodology on which further statistical analysis and pattern classification (e.g., clustering of motion vectors according to angle distribution, speed distribution) is based.

### Quantification of fluorescence signal between frame 44-72 in the presence of antibiotics

Standardize Fluorescence intensity was derived by a pipeline created on top of time-lapse microscopy videos. The videos were preprocessed to extract the area of interest and de-noised of any background option. Frame indices were synchronized in datasets and pixel-wise values of intensity were averaged at the frame level. Minimum max scaling was applied to the signals to make them comparable. Frames 44-72 were chosen to collect the intermediate cellular responses without pre-stabilization and end saturation. Such a strategy allowed making a direct comparison of the temporal signal trends in the conditions of the experiment.

## RESULTS

### Clustering outcomes from GMM analysis

GMM applied to the data on the motion of bacteria was able to cluster the vectors of displacement into different behavioral clusters successfully. Figure 1A indicates that under the general conditions, the clustering provided three groups Cluster 1 (blue), Cluster 2 (orange), and Cluster 3 (green) centred around the origin with moderate spread. This distribution indicates the combination of the motile and non-motile bacterial population.

In PMB treatment the clustering behavior was changed significantly. Figure 1B shows the GMM clustering of the motion data of PMB-treated samples specifically. In this case, there were two clusters formed,

namely PMB Cluster 1 (green), which is closely packed around the origin, and PMB Cluster 2 (orange), which is more widely spread. Such decrease of cluster diversity and the concentration of vectors around zero motion reveals that PMB has an inhibitory impact on the motility of bacteria.

### Directional motion analysis

Directional vector plots were created in order to further interpret the nature of bacterial movement. The motion vectors of each cluster are depicted in figure 1C and radiating towards the origin and colored by cluster identity. Individual displacements of the bacteria are depicted in the arrows, whereas the bold black arrow shows the average direction of movement of a specified cluster.

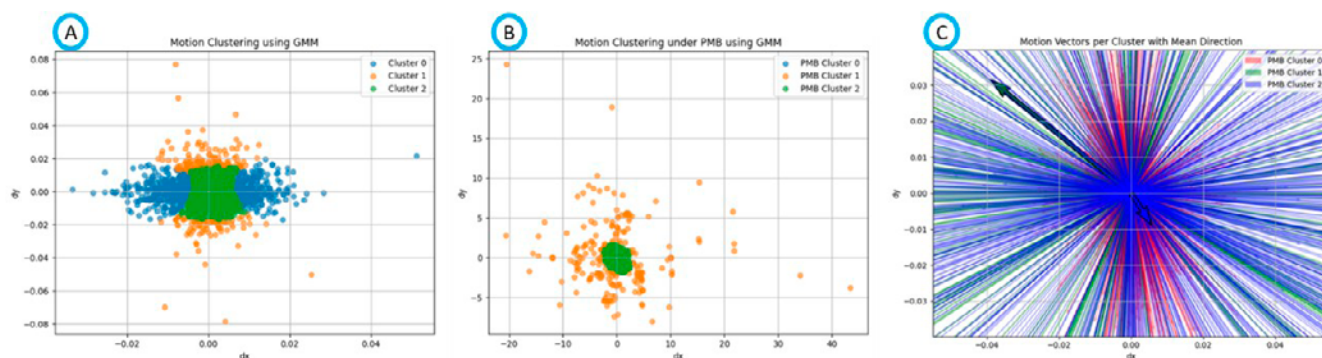


**Figure 1:** A: Motion clustering using GMM clustering of motion features under general conditions. B: Motion clustering under PMB of motion vectors ( $dx$ ,  $dy$ ) using GMM after projection onto principal motion directions. C: Motion vectors per cluster in mean direction visualization, with arrows indicating average movement direction.

The visual pattern indicates that the largest majority of vectors are short and scattered and have no particular orientation. This implies random or suppressed motion, which is in agreement with a stress produced by antibiotics. The average vectors were fairly low and this supports the view that PMB suppresses coordinated motility.

### Statistical description of cluster attributes

Statistical properties of each cluster were calculated in order to measure displacement behavior. These are the mean and standard deviation of horizontal ( $dx$ ) and vertical ( $dy$ ) motion, and the number of vectors in a cluster. The findings are tabulated below as shown in Table 1 below:

**Table 1.** Statistical Summary of Motion Clusters under PMD Summary of displacement statistics for each cluster after PMD-based GMM clustering

Cluster	Mean $dx$	Mean $dy$	Std. $dx$	Std. $dy$	Count
0	0.000227	-0.00074	0.008082	0.015913	2320
1	-0.35396	0.286626	7.424877	4.245224	208
2	0.051807	-0.08105	0.807179	0.565111	715

The variables  $dx$  and  $dy$  (pixels/frame) represent horizontal and vertical components of bacterial motion, respectively.

These values affirm that Cluster 0 is close to statically behavior, whereas Cluster 1 and Cluster 2 are more variable and move more, and perhaps represent subpopulations that resist partially, or exhibit remaining motility.

### Biological interpretation

The clustering and the analysis of the vectors are all pointing to the fact that PMB treatment significantly causes the decrease in bacterial motivity. The prevalence of low-displacement clusters and the lack of directional bias suggest that PMB destabilizes which can be by damaging membranes or inhibiting metabolism. The existence of a more spread cluster (Cluster 2) could indicate some of the bacteria that remain active or adjust in a specific manner. Nevertheless, these findings are to be cross-compared with other data points to ensure biological relevance that include MIC values, exposure time, and viability tests employing fluorescence.

The movement of each bacterium between successive frames is described by each of the vectors, which has both the horizontal (dx) and vertical (dy) components. GMM was used to cluster these vectors in order to determine motion patterns. Each cluster was then plotted directionally to create an image of the mean movement and distribution.

Figure (2) shows seven directional vectors of the movement of bacteria in two antibiotic courses in terms of Ampicillin and PMB. The subplots were linked with the three distinct experimental videos respectively, and the vectors were categorized into three different groups, with respect to the behavior of displacement. The ampicillin-treated samples and the PMB-treated samples are represented in the upper layer (Figure 2A 2D) and the lower layer (Figure 2E 2G), respectively. The vectors are projected surrounding the origin and the density, length and direction signify the extent and direction of the bacterial movements. The motility pattern patterns

of the three treatments can be analyzed and it is seen to have distinct clustering patterns with mean speed and SD of each cluster.

In ampicillin video 1 (Figure 2A), the majority of the vectors are short, and they are concentrated around the origin. Cluster 0 is the dominant one with the mean speed of 0.0021 which implies a high level of inhibition. Cluster 2 is a little more active at 0.1288 although there is a general lack of motion. Ampicillin video 2 (Figure 2B) shows noticeable contrast: Cluster 1 demonstrates a mean speed of  $2.4950 \pm 2.8976$ , which suggests unpredictable movement presumably because of resistance or disruption of the walls. Cluster 0 is suppressed to 0.0052, which points to the heterogeneity of response.

Figure 2C: ampicillin video 3 shows a mixed profile. Cluster 1 has high motility of 0.9664 and Cluster 0 is almost static 0.0054. Cluster 2 lies in the middle at 0.1421, which indicates some inhibition. This trend is reflected in ampicillin video 4 (Figure 2D) where Cluster 1 has high motility at 0.8204, and Cluster 0 is repressed at 0.0058. These findings indicate that population treated by Ampicillin has a large spectrum of response, with full inhibition to active motility.

The samples with PMB treatment display higher uniform suppression. Cluster 1 in PMB video 1 (Figure 2E), has been found to be highly motile with a value of 1.1139 whereas Cluster 2 is almost stationary with a value of 0.0018. In Figure 2F, PMB Video 2, Cluster 2 is transitioning, having a middle activity of 0.5550 and Cluster 0 of 0.0022. Figure 2G (PMB Video 3) is a continuation of this pattern as Cluster 1 is moderately motile with 0.4629 and Cluster 0 is low with 0.0052.

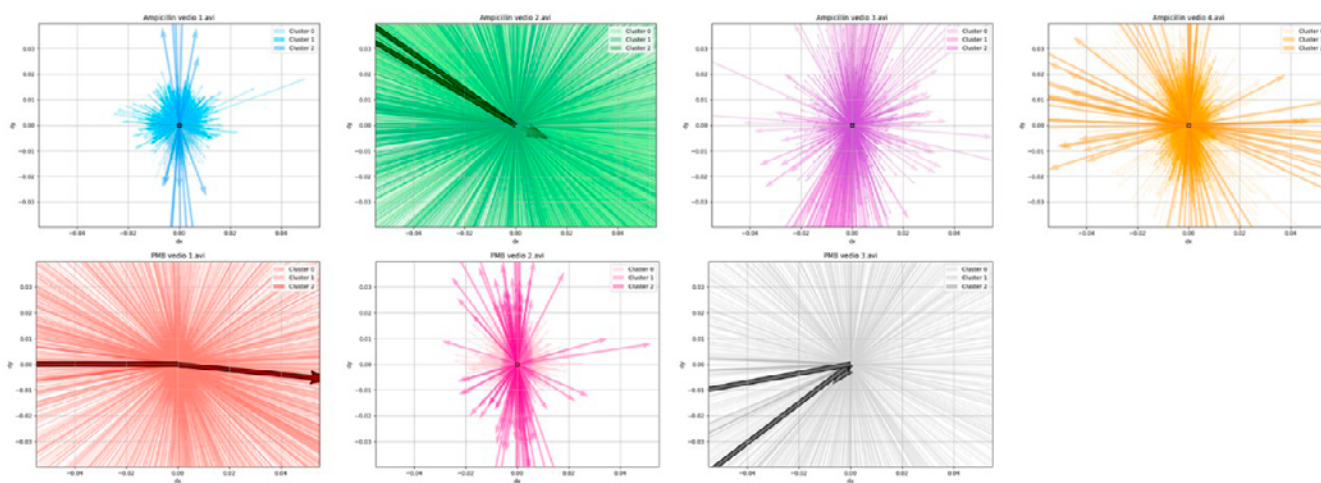


**Figure 2.** Clustered directional displacement vectors of bacterial motion under ampicillin and polymyxin B Treatments. A–E show displacement vector clustering results from four ampicillin-treated bacterial videos. F–G show clustering results from three (PMB)-treated bacterial videos.

Such trends indicate that PMB has a less selective inhibitory impact than Ampicillin.

To reinforce this meaning Table (2) provides a summary of the fastest and slowest mean speeds in every video, with the distinction between active and suppressed clusters. The table shows that there is more variability to Ampicillin treated samples in motility with some of the clusters attaining speeds of more than 2.4 whereas PMB treated samples are more uniform in their suppressing activity with the low-speed clusters prevailing.

**Table 2.** Comparative summary of high-speed and low-speed clusters across experimental videos

Video	Antibiotic	High-Speed Cluster (Mean Speed)	Low-Speed Cluster (Mean Speed)
PMB Video 1	PMB	Cluster 1 (1.1139)	Cluster 2 (0.0018)
PMB Video 2	PMB	Cluster 2 (0.5550)	Cluster 0 (0.0022)
PMB Video 3	PMB	Cluster 1 (0.4629)	Cluster 0 (0.0052)
AmpicillinVideo 1	Ampicillin	Cluster 2 (0.1288)	Cluster 0 (0.0021)
AmpicillinVideo 2	Ampicillin	Cluster 1 (2.4950)	Cluster 0 (0.0052)
AmpicillinVideo 3	Ampicillin	Cluster 1 (0.9664)	Cluster 0 (0.0054)
AmpicillinVideo 4	Ampicillin	Cluster 1 (0.8204)	Cluster 0 (0.0058)

### Comparative angular motion patterns under ampicillin and PMG conditions

Angular distributions around the Z-axis of ampicillin-treated units (1–4) are strongly directionally biased, particularly in Clustering 1 and 2, indicating that ampicillin-induced structured movement or environmental

gradient action. The Y-axis displays more generalized and overlapping curves which denote variable and less controlled motion whereas the X-axis is scattered and biologically not restricted.

Comparatively, there is a more balanced and uniform distribution of PMG units (5-7) along the Z-axis with less directional bias. The Y-axis presents less jagged and more regular trends with improved class reparability, but the X-axis shows two peaks of classes, indicating unstable or oscillating behavior which is probably associated with antibiotic stress. All in all, Figure (3) reveals clear dynamics of motion between the two groups. These disparities drive the emphasis on the impact of antibiotic exposure and environmental circumstances on bacterial movement and classification capabilities.

### Cluster separation and angular response under antibiotic treatment

Scatter plots of four clusters identified under both ampicillin and PMB conditions were presented in Figure 4A–D, which was based on the analysis of motion vectors. The difference in density and dispersion among clusters implies different behavior of the bacteria which might be due to the nature and level of exposure to antibiotics.

Figure 4E and 4F show scatter plot of unclassified or ambivalent clusters. These distributions are seen to be more diffusive and overlapping suggesting transitory motion states or noise-dominated behaviour which was not subject to the primary clustering structure. This pattern can be indicators of intermediate responding to the treatment or mixed motility populations.

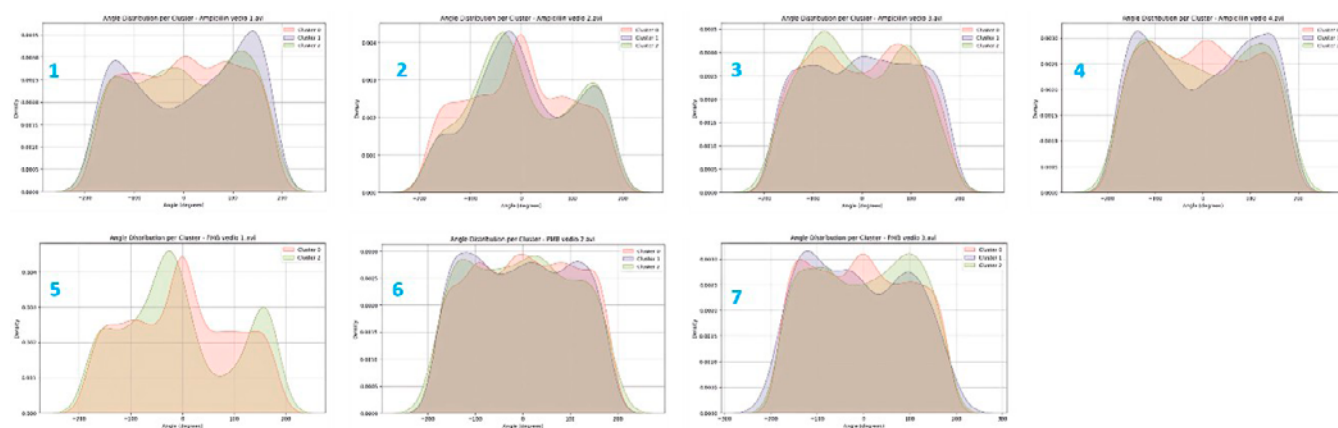


**Figure 3.** Angular density distributions across experimental units and axes under antibiotic treatment. This figure compares angular motion profiles across seven experimental units under ampicillin (Units 1–4) and PMG (Units 5–7) treatments. Ampicillin units show sharper peaks and clearer class separation along the Z-axis (Units 1 and 4), while Y- and X-axis plots (Units 2 and 3) reveal broader or scattered distributions, indicating variable or unconstrained motion. PMG units display smoother, more homogeneous curves with reduced directional bias, though Unit 7 shows double-peaked patterns suggestive of oscillatory movement.

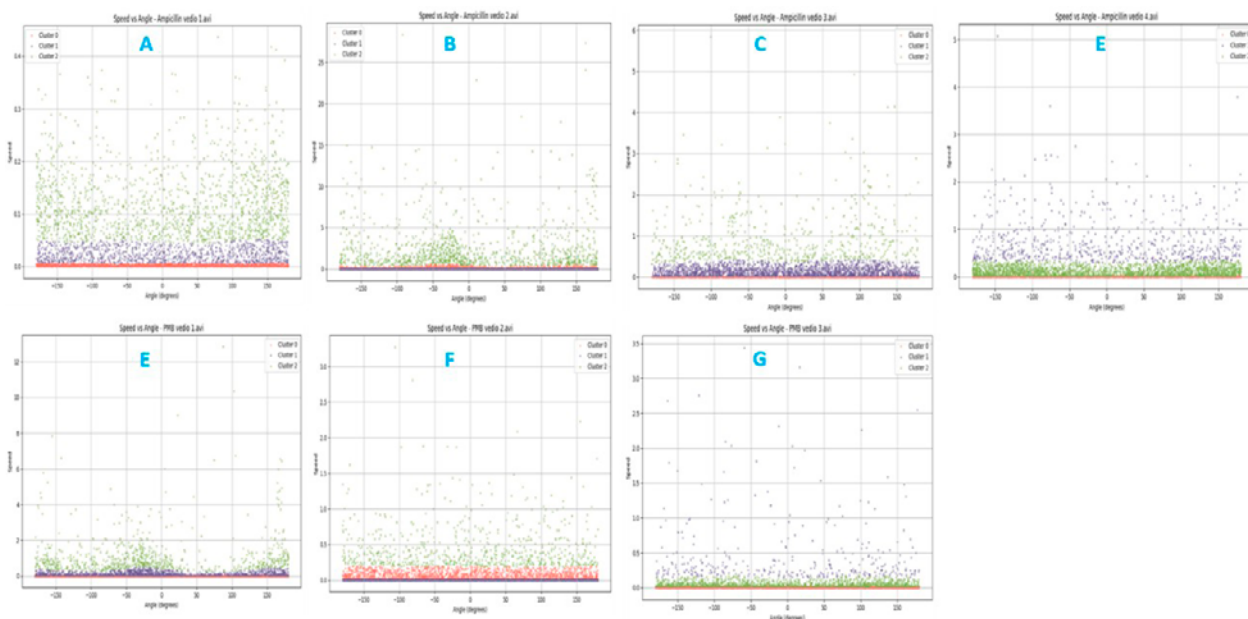


**Figure 4.** Cluster-based motion patterns and angular responses under ampicillin and PMB treatments. (A–D) Scatter plots of four primary motion clusters showing distinct spatial separation under antibiotic exposure. (E–F) Unclassified clusters with diffuse, overlapping distributions indicating transitional or noisy motion states. (G) Spectral angle correlations across 100 biological clustering revealed differential orientation responses to ampicillin and PMB.

Figure 4G shows the correlations of the spectral angles between 100 biological classes between angular motion features of ampicillin and PMB treatments. The angular similarity variation indicates the different reactions to the antibiotics where certain classes possess a high directional alignment and others differ significantly. This implies that every antibiotic has a unique effect on motion orientation, which may represent bias in mechanism of action, bacterial resistance, or stress-induced changes in motility.

**Fluorescent Optical Flow Analysis of Cellular Responses to ampicillin and PMB**

In Figure (5), seven panels (A–G) are acquired by the fluorescence microscopy to compare cellular reactions in these two media conditions, namely; Ampicillin (panels A–D) and PMB (panels E–G). Cells were stained with DAPI (47, 6-diamidino-2-phenylindole), which combines with DNA to generate blue fluorescence and with Alexa 594, which combines with cytoplasmic components, generating pink-red fluorescence. This two-color staining allows a chance to evaluate the distribution and activity of cells in detail.

There are uneven cell density and fluorescence intensity in panels (A– D) that are used to represent cells cultured with ampicillin. In Panel A, there are low cell densities with a low cytoplasmic stain and nuclei

stain with blue stain, indicating low activity. In panel B, there is a marked contrast with thick populations of cells, high staining of the nucleus, and high fluorescence of pink color, which depicts high protein levels and possible mitosis. The panels C and D are similar to panel A, but scattered cells and weaker signal may be due to heterogeneity of response or differences in time points of imaging.

Panels (E– G) of PMB-treated samples show a less irregular and less intense profile of fluorescence. In panel E, the cell distribution is very dense with saturated blue stain nuclei and uniformly spread pink stain which is expected of a regulated or therapeutic cellular response. Panel F and G had a low density of cells and low fluorescence density, which indicates quiescence or dormancy induced by antibiotics. Scale bar Panel G has a spatial reference scale bar.

On the whole, the photographs indicate that the media treated with ampicillin increases cellular activities more so in panel B as compared to PMB-treated samples, which promote a more balanced and controlled response. These findings underscore the media composition effects on cell behavior and can be used in applications of growth stimulation and therapeutic modulation.

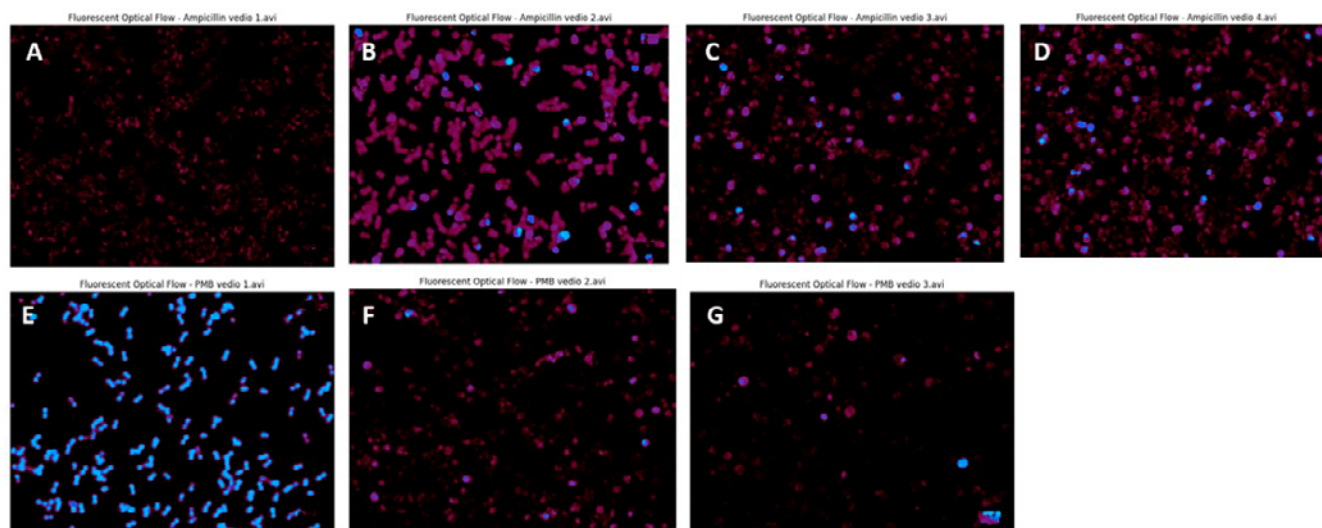


**Figure 5.** Fluorescence microscopy images of cells cultured in ampicillin- treated media (panels A–D) and PMB-treated samples (panels E–G). Nuclei are stained with DAPI, which emits blue fluorescence, and cytoplasmic components are labeled with Alexa 594, emitting pink-red fluorescence. Ampicillin-treated media induces variable clustering and elevated fluorescence intensity, especially in panel B, while PMB-treated samples results in more uniform distribution and moderate signal levels. Panel G includes a scale bar for spatial reference.

### Temporal divergence in fluorescence profiles under antibiotic stress

Figure (6) shows the dynamics of the fluorescence signal between the 44-72 frames indicate that there are differences in response to the treatment of ampicillin and PMB in different concentrations. The ampicillin-treated samples will tend to exhibit slow or intermittent rise in the fluorescence intensity which implies long-term cellular activation or adaptive response to stress. Markedly, the ampicillin video 1 (2x) and Video 3 (3x) has a constant upward trend whereas video 2 (2x) has had a decreasing and then an increasing pattern, which shows a temporary inhibition.

On the contrary, PMB-treated samples are more heterogeneous. PMB Video 3 (4x) displays steady gain of signal whereas PMB video 2 (2x) and video 3 (5x) indicates that there are various paths with sharp fall and partial recoveries of signal, indicating variability in cellular responses or subpopulation effects. These findings of Figure 6 underscore the difference in effect of antibiotic type and concentration of antibiotic on fluorescence signal behavior with time.

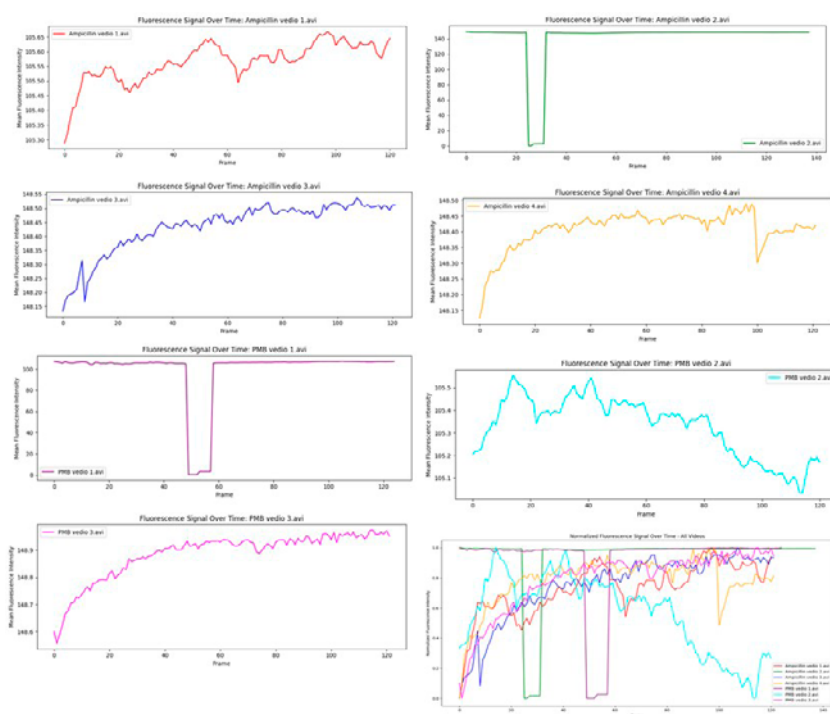


**Figure 6.** Fluorescence signal dynamics between frames 44–72 under ampicillin and PMB treatments. Time-resolved fluorescence intensity profiles for bacterial samples exposed to ampicillin and PMB at varying concentrations. Each graph represents a distinct condition, labeled by antibiotic type, video number, and concentration. Signals were extracted from time-lapse microscopy and normalized using min-max scaling. The analysis focuses on frames 44 to 72, capturing mid-phase cellular responses.

Elevated fluorescence intensity in Cluster 1 correlates with increased motility, suggesting a link between metabolic activation and mechanical response.

## DISCUSSION

It will be demonstrated in this study that the behavior of bacteria under the stress of antibiotic is studied in depth by applying it to the cases of combined optical flow, clustering, and angular profiling methods. The results show that ampicillin and polymyxin B (PMB) induce various motility responses in which ampicillin-treated samples generate mixed motility responses whereas PMB-treated samples give consistent motility responses. The vector-based clustering of displacement as well as the angular density distributions along spatial axes are both used to complement these findings by displaying that there is a modulation of bacteria behavior in response to antibiotics.

Motility under ampicillin treatment was very diverse in forms of motion clustering. Particularly, cluster 1 exhibited the tendency to be large in the average speeds up to 2.4950 pixels/frame with ampicillin video 2, but cluster 0 was practically immobile in all the samples. This could suggest that ampicillin has a bifurcated action, which can reflect more or less cell wall disruptive or resistance action in subpopulations. This was unlike the PMB-treated samples in which there was even suppression and low-speed clusters dominated with only a few examples of high motility. These results support the finding of previous studies that have indicated PMB of the outer membrane integrity which leads to a rapid immobilization of Gram negative bacteria<sup>18,19</sup>.

These variations are also supported with the consideration of angular motion where ampicillin-treated units it was found to be severely directionally biased along the Z-axis particularly in cluster 1 and cluster 2 indicating that there must have been some orderly movement that may have been due to chemotactic escape behavior or mechanical response. The distributions of the Y-axis were wider and crossed over that denoted less restricted motions whereas the X-axis profiles were scattered and unrestricted biologically. The units treated with PMB, in their turn, were less angularly distributed and smoother and more symmetrical, less directional and more distinct classes were viewed along the Y-axis. Such observations are consistent with the findings of the studies pointing to the fact that PMB triggers envelope stress responses which inhibit coordinated motility<sup>20,21</sup>.

Additional pixel-level-dynamics was observed when the HSV-encoded dense motion mapping (HEDMM-FBOF) was integrated. In ampicillin-treated samples, there was heterogeneity in color patterns with red and pink colorations indicating horizontal and rotational movement, whereas in PMB-treated samples there was uniformity of color patterns with blue and cyan colors indicating vertical movement and dormancy respectively. This visualization tool provides a new way of understanding how bacteria react to stress and helps to supplement classical analysis which is based on vectors.

In comparison to the past research, our methodology has a number of novelties. Although previous studies have described the effect of antibiotics on motility as a bulk effect or qualitative observation under the microscope<sup>22-25</sup>, the current research uses quantitative clustering and angular profiling measures across axes and conditions. The application of GMM to divide motion vectors into biologically significant clusters enables a strict distinction of motile, stressed and stationary populations. Besides, correlation of spectral angle over 100 biological classes gives a high-resolution measure of directional response comparison which is not considered in previous literature<sup>5,26</sup>.

Interestingly, we have differing results with previous literature which propose homogenous suppression with 20 -lactam antibiotics. As an example, Fuglesang and Bergan have found that *E. coli* motility was always inhibited in the presence of ampicillin during the simulated *in vivo*<sup>27</sup>, but our results indicate that there is a high level of variance, with some clusters retaining high motility. This variation can be explained by the variations in the imaging resolution, strain selection, or concentration of antibiotics. On the same note, although Benisty et al. found an abnormal swarming of the insects when subjected to sublethal exposure to antibiotics<sup>28,29</sup>, our findings also reveal organized angular response under suppressive conditions, and it is possible that directional movement may be preserved in resistant subpopulations.

These findings are biologically relevant as evidenced by the results of fluorescence microscopy. Sample treatment with ampicillin produced inconsistent nuclear and cytoplasmic staining with panel B presenting strong nuclear and cytoplasmic signals that suggest metabolic activation. Samples to which PMB was added, on the one hand, exhibited homogenized and less intense fluorescence the opposite of which is an indication of dormancy or regulated reaction. The findings also show

that the motility patterns are linked with the cellular activity and may be adopted as the surrogates of the antibiotic activity<sup>30,31</sup>.

Notably, the article has provided a two-modality model of mechanical phase noise detection and optical motion tracking. This enables simultaneous vibrational and visual displacement measurements at the nanoscale which is a powerful tool and can assist in real time monitoring of the bacterial response. This is a practice that has not been stated previously and can be applied in order to direct the further diagnostic platform or antimicrobial screening tests.

Irrespective of these strengths, there are a number of limitations that should be noted. First, the unsupervised algorithms used in the clustering can be very sensitive to the choice of parameters and noise. Second, the analysis is restricted to two antibiotics and one bacterial strain making it hard to generalize. Third, angular profiling is not an ideal method as it fails to record intracellular behavior or biochemical signaling pathways. Further research must include the multi-strain comparisons, increase the antibiotic panel and include transcriptomic or proteomic data to clarify the mechanisms behind it.

## CONCLUSIONS

The paper presents a new multimodal system to examine the behavior of bacteria under the influence of antibiotic stress, which incorporates the use of clustering algorithms, angular profiling through spatial axis, and the use of HSV-based visualization of dense motions. In contrast to the earlier studies, which based their findings on bulk motility metrics or qualitative microscopy, our method allows high-resolution separation of the motile subpopulations and directional motility, which showed antibiotic-specific motility patterns. The fact that the structured angular responses and spectral class reparability in the presence of ampicillin occur in the presence of inhibitory conditions is a phenomenon that has not been reported before. Moreover, fluorescence imaging combined with motion clustering can give a biologically understandable correlation between cellular motion and mechanical motion. The innovations provide a fresh insight on the understanding of bacterial adaptation and it might serve in developing diagnostic tools addressing resistance profiles in the future. Further studies ought to expand this model to other strains and antibiotic classes, and determine how

these models can be applied to other clinical microbiology and real-time antimicrobial screen translational potential.

**Ethics Statement and Conflict of Interest Disclosures**  
Financial support and sponsorship: All authors have declared that no financial support was received from any organization for the submitted work.

This study was approved by the Institutional Research Board and Ethics Committee.

**Conflict of interest:** No known conflict of interest correlated with this publication.

**Availability of data and materials:** The data used and/or analyzed throughout this study are available from the corresponding authors upon reasonable request.

**Competing interests:** The authors declared that they have no competing interests.

**The use of generative AI and AI-assisted technologies:** The authors did not use in this article generative AI and AI-assisted technologies.

## REFERENCES

- Brand C, Newton-Foot M, Grobbelaar M, Whitelaw A. Antibiotic-induced stress responses in Gram-negative bacteria. *J Antimicrob Chemother.* 2025;80(5):1165–84.
- Palma V, Gutiérrez MS, Vargas O, Parthasarathy R, Navarrete P. Methods to evaluate bacterial motility and its role in bacterial-host interactions. *Microorganisms.* 2022;10(3):563.
- Bardy SL, Briegel A, Rainville S, Krell T. Recent advances in bacterial locomotion and signal transduction. *J Bacteriol.* 2017;199(18):e00203–17.
- Abbas SH, Kiani HS, Gohar F, Zahra S, Javed A, Khan S, Khan D. Understanding the role of bacterial biofilm in antibiotic resistance. *IntechOpen.* 2025.
- Sen S, Vairagare I, Gosai J, Shrivastava A. RABiTPy: an open-source Python software for rapid, AI-powered bacterial tracking. *BMC Bioinformatics.* 2025;26:127.
- Zabn M, Dawood AA. Bacterial Acoustic Fingerprinting: Nanomotion and Spectral Feature Analysis Between Real and Synthetic Oscillations Using Deep Neural Networks. *J Chem Health Risks.* 2025; 15(4): 990–1002. Liu M, Yang W, Zhu W, Yu D. Innovative applications of bacterial biosensors in medicine. *Front Microbiol.* 2025;16:1507491.
- McGoverin C, Steed C, Esan A, Robertson J, Swift S, Vanholsbeeck F. Optical methods for bacterial detection and characterization. *APL Photonics.* 2021;6:080903.
- Dawood A.A. Designing an immuno-epitope candidate vaccine from (Opa, ProA, ProB, RmpM and BamD) proteins against *Neisseria gonorrhoeae* and *Neisseria meningitidis*. *Vacunas.* 2024;25(4): 481–491
- Dawood A. Identification of Cytotoxic T cell and B-cell

- epitopes in the Nucleocapsid Phosphoprotein of COVID-19 using Immunoinformatics. *Microbiol J.* 2021; 83(1): 78-86. doi: 10.15407/microbiolj83.01.078.
10. Pepino R, Tari H, Bile A, Nabizada A, Fazio E. Optical bacteria recognition via cross-polarized scattering. *Symmetry.* 2025;17(3):396.
  11. Ramos J, Nedjah N, Mourelle LM. Crowd anomaly detection using optical flow and artificial bacteria colony optimization. *ICCSA.* 2017;10405:329-344.
  12. Codex Yubetsu. Quantifying and minimizing errors in 2D and 3D tracking of bacterial motion. *Yubetsu Codex.* 2023;1(1):cef9f368.
  13. Dawood AA, Al Hadidi EW, Alnori HA. Structural and molecular insights into AipA and OmpA: key drivers of *Anaplasma phagocytophilum* host cell invasion. *Medicina Moderna.* 2025;32(3):249-61. doi:10.31689/rmm.2025.32.3.249.
  14. Piskovsky V, Oliveira NM. Bacterial motility governs dynamics of antibiotic resistance evolution. *Nat Commun.* 2023;14:41196.
  15. Johnson WL, France DC, Rentz NS, Cordell WT, Walls FL. Sensing bacterial vibrations and early response to antibiotics with phase noise of a resonant crystal. *Sci Rep.* 2017 Sep 22;7(1):12138. doi: 10.1038/s41598-017-12063-6.
  16. Abdelmalek I, Svahn I, Mesli S, Simonneaux G, Mesli A. Formulation and microbiological activity of ampicillin microspheres. *J Mater Environ Sci.* 2014;5(6):220-30.
  17. Davis E. Analysing ampicillin conformational ensembles using molecular dynamics. *Mol Biol Open Access.* 2024;13(4):449.
  18. Nazwar TA, Saputra BR, Retnoningsih D, Bal'afif F, Wardhana DW. Prevalence and antibiotic resistance of bacteria isolated from cerebrospinal fluid of neurosurgical patients in Malang, Indonesia. *Modern Medicine.* 2023;30(4):341-347.
  19. Dawood A.A. The impact of magnesium sulfate on the gene expression of *Bordetella pertussis* (ptxP1 and ptxP3) strains and the incidence of whooping cough in Nineveh. *Vacunas.* 2024;25(2): 214-223.
  20. Al-Waely H, Al-Ahmer S. Evaluation of the role of some microRNAs in coronavirus-19 infection in a sample of Iraqi patients. *Modern Medicine.* 2024;31(3):237-242. doi:10.31689/rmm.2024.31.3.233.
  21. Pan H, Zhang Y, He GX, Katagori N, Chen H. Quantification of bacterial cells after nanoparticle exposure. *BMC Microbiol.* 2014;14:222.
  22. Bhattacharya M, Das A, Khatun R, Sengupta S. Advances in bacterial classification: from phenotypic traits to genomic signatures. *IJPS.* 2025;3(5):IJPS/250304739.
  23. Abd Al-Razak M, Al-Saadi B, Al-Saedi A. Evaluation of the role of two SNPs in MTHFR gene polymorphisms (rs1801133 677 C>T and rs1801131 1298A>C) with homocysteine level in Iraqi patients with chronic kidney disease. *Modern Medicine.* 2024;31(3):227-232. doi: 10.31689/rmm.2024.31.3.227.
  24. Wang P, Sun H, Yang W, Fang Y. Optical Methods for Label-Free Detection of Bacteria. *Biosensors (Basel).* 2022 Dec 15;12(12):1171. doi: 10.3390/bios12121171.
  25. Su XL, Li Y. Quantum dot biolabeling coupled with immunomagnetic separation for detection of *Escherichia coli* O157:H7. *Anal Chem.* 2004 Aug 15;76(16):4806-10. doi: 10.1021/ac049442+.
  26. Dawood A. A Method Utilizing an Image Visibility Graph to Portray the Arrangement of Genomic Data Sequencing, Gene Frequencies for The Peptidoglycan-Associated Lipoprotein (Pal) Gene in *Brucella* Spp., and Prevalence of Brucellosis in Nineveh. *Moderna Med.* 2024; 31(2): 155-165. doi: 10.31689/rmm.2024.31.2.155.
  27. Fuglesang JE, Bergan T. Antibacterial kinetics of ampicillin against *E. coli* under simulated in vivo conditions. *Infection.* 1982;10(1):39-45.
  28. Benisty S, Ben-Jacob E, Ariel G, Be'er A. Antibiotic-induced anomalous statistics of bacterial swarming. *Phys Rev Lett.* 2015;114(1):018105.
  29. Idil N, Aslyüce S, Perçin I, Mattiasson B. Recent Advances in Optical Sensing for the Detection of Microbial Contaminants. *Micromachines.* 2023; 14(9):1668. <https://doi.org/10.3390/mi14091668>.
  30. Guliy OI, Bunin VD. Electro-optical analysis as sensing system for detection and diagnostics of bacterial cells. In *Biointerface engineering: prospects in medical diagnostics and drug delivery 2020*; (pp. 233-254).
  31. Horváth R, Pedersen HC, Skivesen N, Selmeczi D, Larsen NB. Optical waveguide sensor for on-line monitoring of bacteria. *Optics letters.* 2003 Jul 15;28(14):1233-5.